Supporting Information

Rapid dissolution of amyloid β fibrils by silver nanoplates

SWATHI SUDHAKAR, ETHAYARAJA MANI*

POLYMER ENGINEERING AND COLLOID SCIENCE LABORATORY, DEPARTMENT OF CHEMICAL ENGINEERING, INDIAN INSTITUTE OF TECHNOLOGY, MADRAS-600 036, INDIA

ethaya@iitm.ac.in

1. Synthesis of Silver nanoparticles (AgSP)

In a 100 mL round bottom flask, 0.001 M of AgNO3 and 0.004 M of PVP was added and mixture was stirred under room temperature. To the solution, 100 µL of Sodium borohydride (0.187 gm/100 mL) was added dropwise under vigorous stirring.[1] The change in color to bright yellow indicating the formation of AgSP was observed. The resultant solution was centrifuged for 20 min at the speed of 13,000 rpm. UV visible spectroscopic studies implied that the peak at 420 nm caused by surface plasmon resonance phenomenon of the electrons in the conduction band electrons of silver confirms the synthesis of nanoparticles. In addition to that TEM images shown that the particles are in the range of 20 $\pm$ 5 nm.

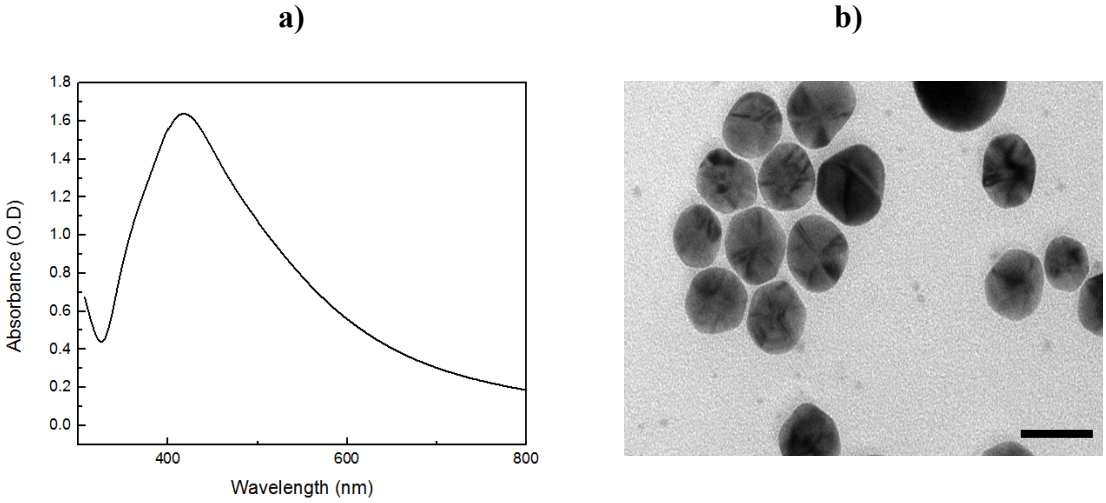

Figure S1: a) UV-Visible spectrum of AgSP b) TEM image of AgSP Scale bar: 20 nm

2. Synthesis of silver nanoplates (AgTNP)

Poly (vinyl pyrrolidone) (PVP, Aldrich, Mw = 40 000) was dissolved in 8.0 mL of water and heated to 60 °C in air for 21 h under magnetic stirring[2]. Meanwhile, 3.0 mL of an aqueous solution of $AgNO_3$ (188 mM) was rapidly added into the vial. The molar ratio used between the PVP and $AgNO_3$ was maintained in 15. Then the mixture was centrifuged at 13,000 rpm for 30 minutes. The samples were characterized by TEM and SEM and the size is in the range of 70 $\pm$8 nm and UV-vis extinction spectra were also taken from aqueous suspensions of the products. Features in the size range of 3 nm in Fig S1 b and S2 b is due to the charging effect of Ag nanoparticle and it was prominently observed by many research groups.[3] In the one-pot

synthesis of AgTNP using PVP, usually, a mixture of AgTNP (~80%) and spheres (~20%) is obtained, as AgTNPs are formed due to spontaneous twinning of spherical particles at the nucleation stage. All the AgTNP samples contained some amount of spherical silver nanoparticles.

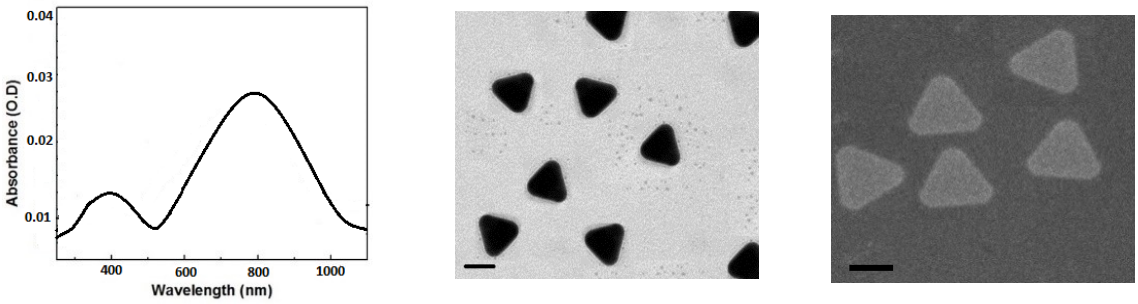

Figure S2: a) UV-Visible spectrum of AgTNP at 30 nM b) TEM image of AgTNP c) SEM image of AgTNP. Scale bar: 50 nm.

3. Quantifying Congored binding to amyloid

The spectrophotometric method as described by Klunk et al[4] was employed to determine the number of moles of congored binding to amyloid fibrils.Briefly, when the amyloid fibrils were added to the Congo red (CR) solutions, hyperchromic effect and the shift in the spectrum was observed in the CR bound amyloid fibrils compared with CR alone (Figure S4) The point of maximal spectral difference occurs at 540 nm. We can see the isosbestic point at 400 nm at which the spectra intersect because both free CR and bound CR and have equal molar extinction coefficients. Molar extinction coefficients were calculated using Beer lamberts law for CR alone and CR bound amyloid fibrils. The equation was derived according to the Klunk et al[4],[5] paper and the concentration of the bound ligand can be found by following equation.

$$C_b = A^{540}/4780 - A^{405}/6830$$

Where A_t is the total absorbance at any wavelength and C_b is the concentration of the CR bound to the amyloid fibrils. The free ligand, C_f, is the difference between the total concentration of CR and C_b. Figure S5 shows the binding curve of CR binding to amyloid fibrils. Scatchard analysis of these data is shown in the Figure S6. The binding reaches saturation, and the maximal binding does not continue to drift up after some point. From the

scatchard analyses shown in Figure S5, it was clear that the B_{max} obtained was 2.64 moles of CR per mole of amyloid fibril molecules and the K_d values was 3.664 x 10^{-7} M. To ensure that AgTNP absorbance does not have any effect in CR absorbance assay, the absorbance for 30 nM AgTNP was compared along with CR absorbance spectrum and it was observed that 30 nM of AgTNP does not interfere with the CR based amyloid fibril detection.

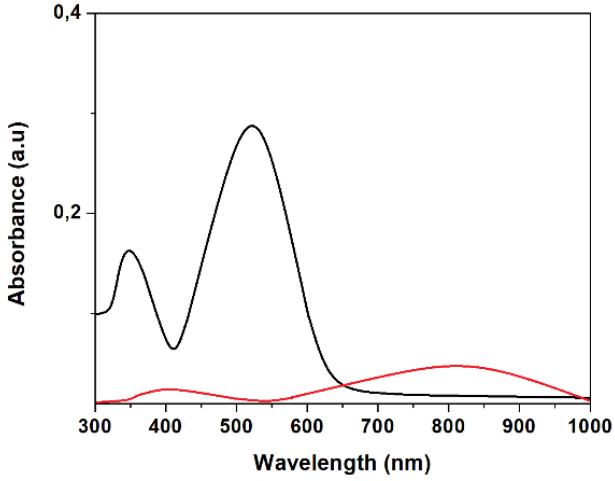

Figure S3: UV-VIS absorption spectra of a 30 µM of Congo red solution (black curve) in 10 µM amyloid fibrils and of 30 nM AgTNP solution (red curve).

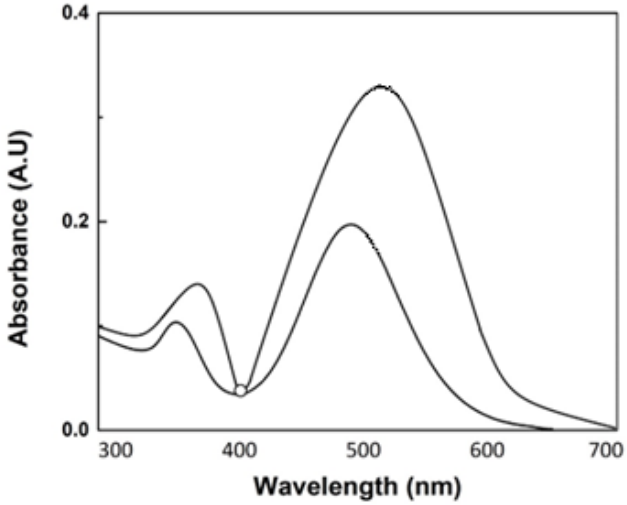

Figure S4: Absorbance spectra of a 30 µM of CR solution with and without addition of (10 µM) amyloid fibrils. From the top the first curve denotes the spectrum of Congo red bound amyloid fibrils. Open circles denote the isosbestic points.

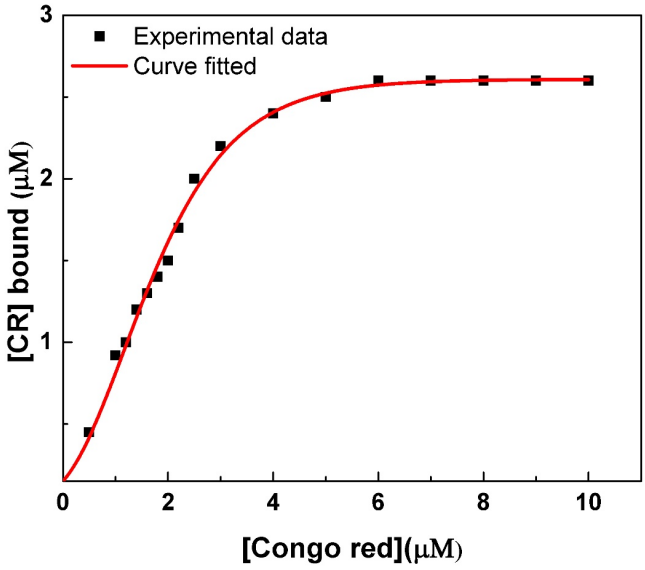

Figure S5: Binding curve of CR and amyloid fibrils by the spectrophotometric method. Various concentrations of CR were incubated with 1 μM of amyloid fibrils. The absorbance at 540 and 405 nm was measured, and CR bound were calculate using above equation. The curves were calculated by sigmoidal fitting.

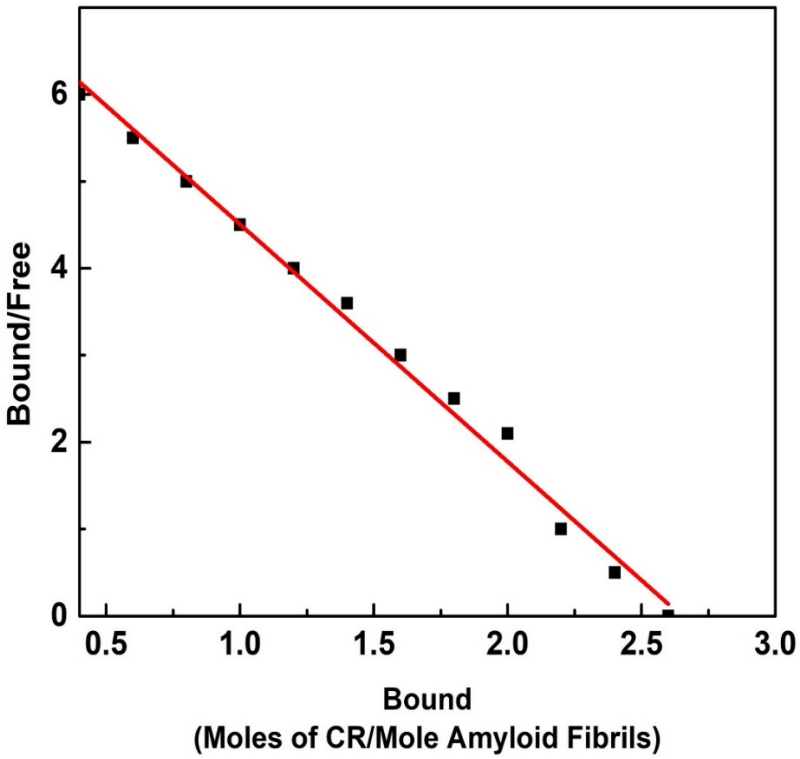

Figure S6: Scatchard analyses of the CR binding to the amyloid fibrils.

Optical microscopic images of the samples shown in Figure S7 illustrate the morphological changes associated with Aβ fibrils treated under different conditions. The pure mature fibrils used in all the studies are shown in Figure S7a indicating optical microscopic images of the entangled Aβ fibrillar network. Figure S7b shows microscopic images of the mature fibril treated with 30 nM of AgSP for 24 h. This figure shows some partial disruption in the fibrillar network indicating partial dissolution induced by AgSP. Figure S13c shows the image of mature fibril sample treated with 30 nM AgTNP for 24 hr and we observe the presence of fibril structures significantly. However, when the sample is treated with 30 nM of AgTNP and illuminated with NIR laser, almost all of the fibrillar structure is transformed to small globular units as shown in Figure d. Although some quasi-spherical structures are found, the fibrils have disappeared, supporting the inference from the Congo red absorbance in Figure 1a.

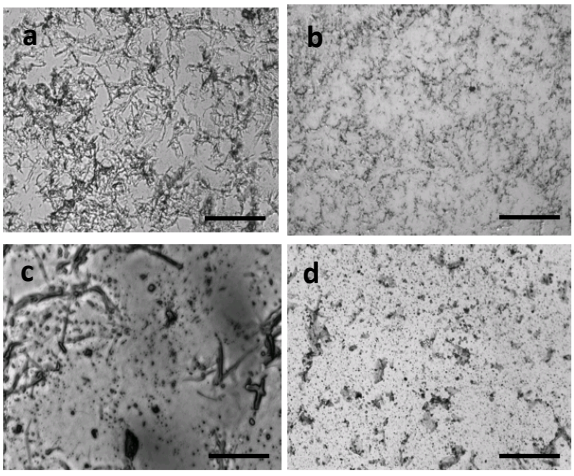

Figure S7. Optical microscopic images of a) preformed fibrils b) fibrils treated with AgSP c) fibrils treated with AgTNP in the absence of NIR irradiation d) fibrils treated with AgTNP in the presence of NIR irradiation. Scale bar: 1 μm.

TEM images of the samples incubated with AgSP of different concentration are shown in Figure S8. Figure S8a shows the presence of mature fibrils entangled throughout the image in the control sample. Figure S8b-f shows the TEM images of the sample incubated with AgSP of various concentration of 3 nM, 6 nM, 8 nM, 10 nM and 30 nM respectively, for 24 h.

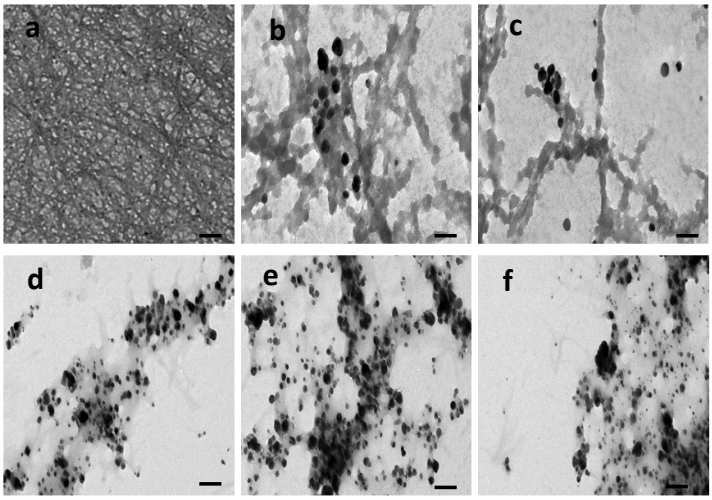

Figure S8. Aβ fibrils were incubated with different concentration of AgSP for 24 h (a) 0 nM (Control) (b) 3 nM (c) 6 nM and (d) 8 nM (e) 10 nM (f) 30 nM. Scale bar: 50 nm

3. Supplementary results

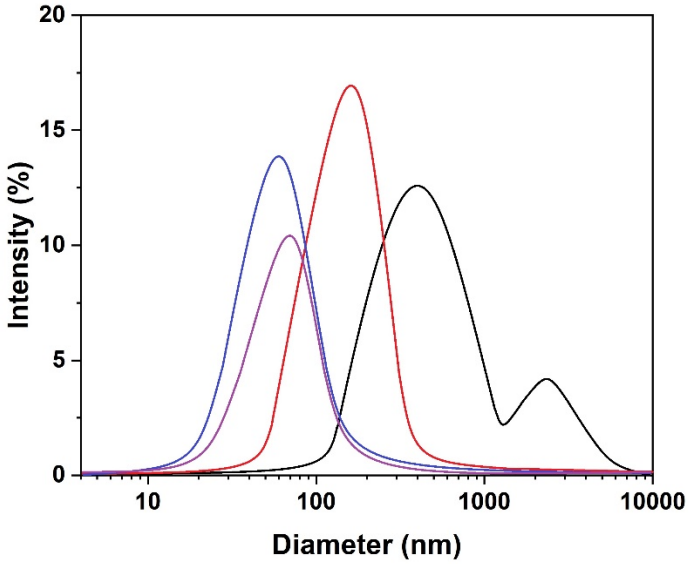

Figure S9: DLS analysis of the Aβ fibril size distributions. Four replicates were performed in each case and the average is shown. Black – mature fibrils; Red- fibrils incubated for 30 min with 30 nM of AgTNPs with NIR irradiation; Blue- fibrils incubated for 60 min with 30 nM of AgTNPs with NIR irradiation; Purple – size distribution of AgTNPs alone after passing NIR without amyloid fibrils.

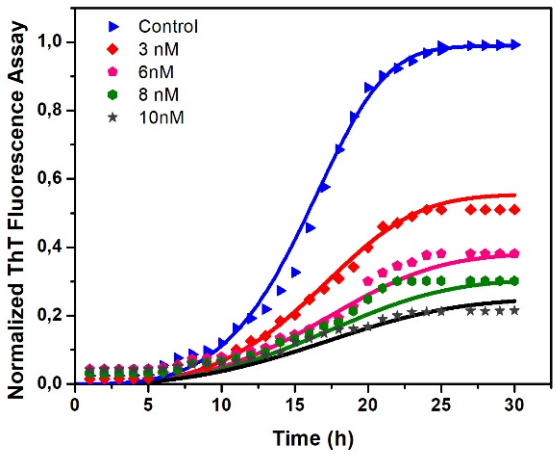

Figure S10. Comparison between model[6] and experiment on the kinetics of fibrillation in the presence of AgTNP.

Table S1. List of parameters used in the kinetic model

Parameter	*Value*
*n**	3
k_1	$8x10^{-3}$ $m^3/(mol.s)$
k_2	$1.3x10^{4}$ $m^3/(mol.s)$
k_{frag}	$1.5x10^{-8}$ s^{-1}
	Silver
p	0.53
k_3	$25x10^{1}$ $(m^3/mol)^p.s^{-1}$
k_4	0.2 s^{-1}

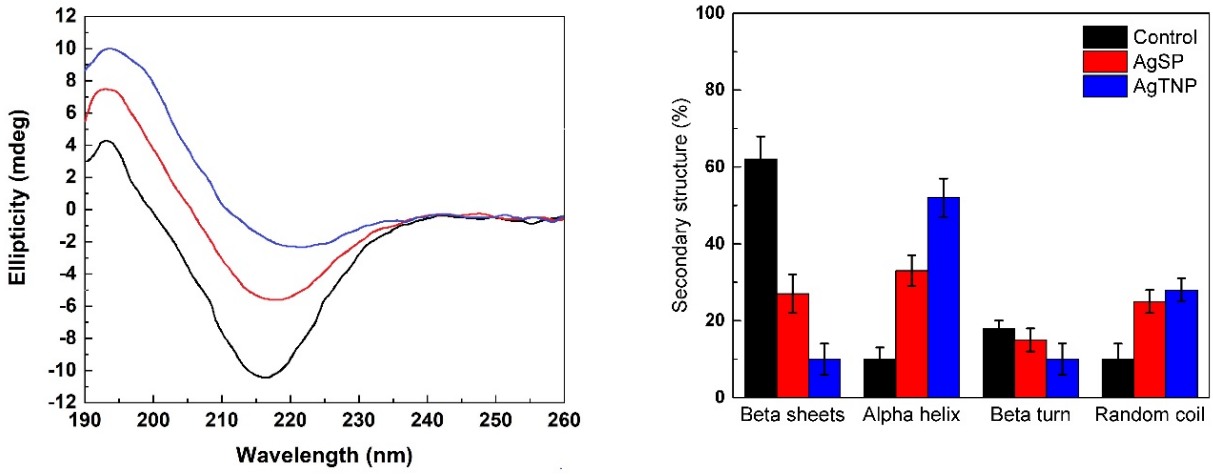

Figure S11: a) The CD spectra show the secondary structures of Aβ aggregates (black) and protein incubated with AgSP (red) and AgTNP (Blue). (b) Secondary structure content of amyloid treated with AgSP and AgTNP of 30 nM concentration for 24h.

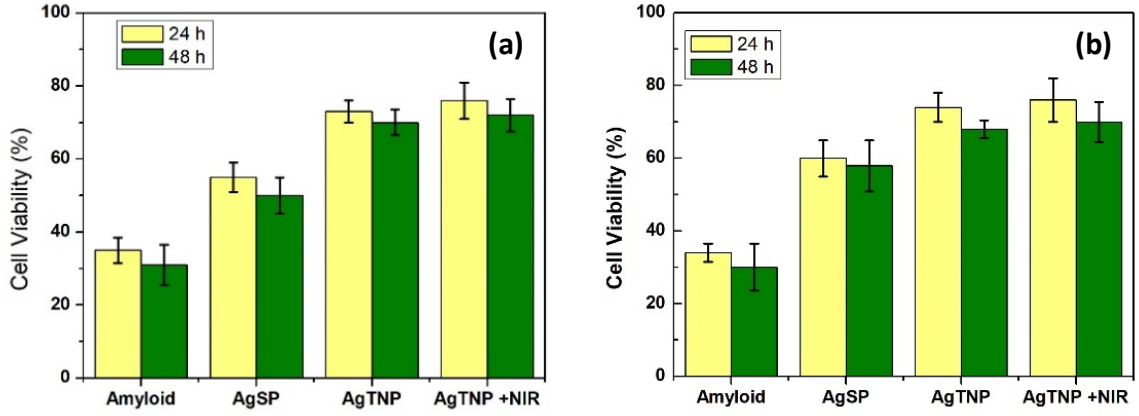

Figure S12. a) MTT assay and b) LDH assay showing the cell viability (percentage) of the BE-(2)-C cells in the solution of amyloid fibrils, treated with AgSP, AgTNP, and AgTNP – NIR illuminated.

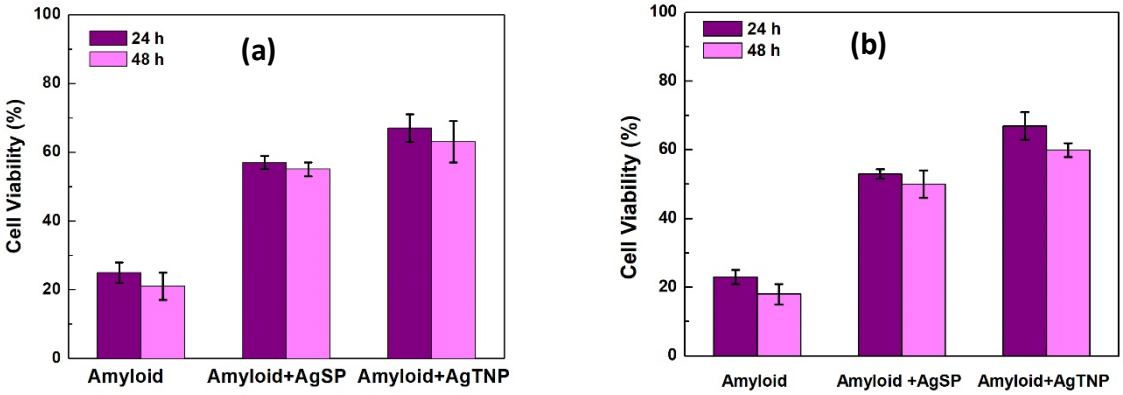

Figure S13. a) MTT assay and b) LDH assay showing the SH-SY5Y cell viability (percentage) in the protein solution treated with 30 nM of AgSP and 30 nM of AgTNP. The data are given for three different incubation times.

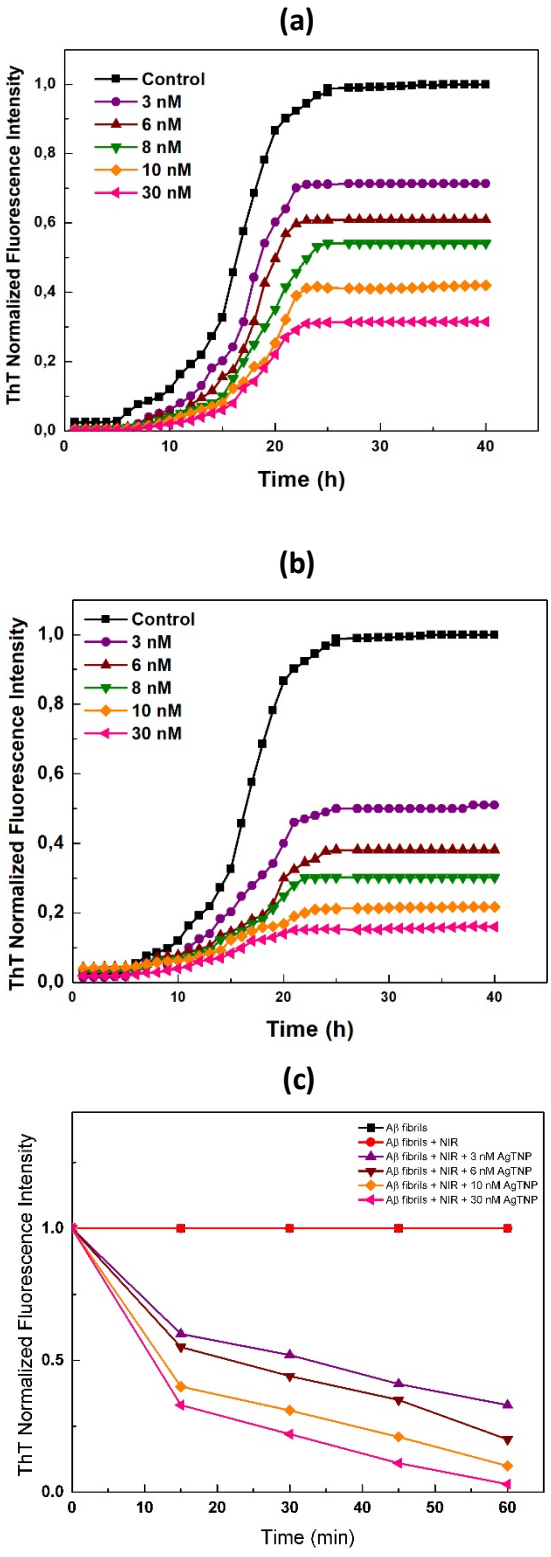

Figure S14: ThT fluorescence intensity of Aβ fibrils incubated with a different concentration of a) AgSP and b) AgTNP. The curve corresponding to control refers to the growth of fibrils in the absence of NP. c) Dissociation kinetics of mature fibrils after passing NIR rays on AgTNP measured in terms of ThT intensity.

References

(1) Kumar, M.; Devi, P.; Kumar, A. Structural Analysis of PVP Capped Silver Nanoparticles Synthesized at Room Temperature for Optical, Electrical and Gas Sensing Properties. *J. Mater. Sci. Mater. Electron.* **2017**, *28* (6), 5014–5020.

(2) Washio, I.; Xiong, Y.; Yin, Y.; Xia, Y. Reduction by the End Groups of Poly(Vinyl Pyrrolidone): A New and Versatile Route to the Kinetically Controlled Synthesis of Ag Triangular Nanoplates. *Adv. Mater.* **2006**, *18* (13), 1745–1749.

(3) Salvioni, L.; Galbiati, E.; Collico, V.; Alessio, G.; Avvakumova, S.; Corsi, F.; Tortora, P.; Prosperi, D.; Colombo, M. Negatively Charged Silver Nanoparticles with Potent Antibacterial Activity and Reduced Toxicity for Pharmaceutical Preparations. *Int. J. Nanomedicine* **2017**, *12*, 2517–2530.

(4) Klunk, W. E.; Pettergrew, J. W.; Abraham, D. J. Quatitative Evaluation of Congo Red Binding with a Beta-Pleated To. *J. Histochem. Cytochem.* **1989**, *37* (8), 1273–1281.

(5) Klunk, E.; Petegrew, J. A. Y. W.; Abraham, J. Two Simple Methods for Quantifying Low-Affinity Dyeâ € ” Substrate Binding ’ the Points. **1989**, *37* (8), 1293–1297.

(6) Ramesh, N. K.; Sudhakar, S.; Mani, E. Modeling of the Inhibitory Effect of Nanoparticles on Amyloid β Fibrillation. *Langmuir* **2018** 34(13), 4004-4012.